SARTORIUS

Application Note

May, 2026

Keywords or phrases:
Extracellular vesicles, mesenchymal stromal cells, ion exchange chromatography, membrane chromatography, downstream processing, Sartobind Convec® D

Scalable Purification of Extracellular Vesicles Using Sartobind Convec® D Membrane Chromatography

Mehdi Dehghani[1], André Krause[2], Franziska Bollmann[2], Swapnil Chaudhari[2]
[1] Sartorius Stedim North America Inc., Bohemia, USA
[2] Sartorius Stedim Biotech GmbH, Göttingen, Germany

Contact: swapnil.chaudhari@sartorius.com

Abstract

Extracellular vesicles (EVs) represent a rapidly growing therapeutic modality for drug delivery and regenerative medicine. However, their commercial translation has been limited by the lack of robust, scalable downstream purification technologies. Conventional resin-based ion-exchange chromatography and ultracentrifugation suffer from low throughput and shear stress, resulting in poor yields and batch variability.

This study demonstrates the application of Sartobind Convec® D, a next-generation weak anion-exchange membrane adsorber, for the purification of mesenchymal stromal cell–derived EVs. Using an optimized analytical and process workflow, we show that Sartobind Convec® D enables efficient depletion of non-vesicular extracellular particles while maintaining high EV recovery, structural integrity, and bioactivity.

At laboratory and pilot scales, Sartobind Convec® D delivered up to 39% particle recovery and > 99% protein and DNA clearance, with linear scalability and short process times. These results position Sartobind Convec® D as a key platform technology for industrial-scale EV purification workflows.

Introduction

Extracellular vesicles as therapeutic platforms

Extracellular vesicles (EVs), including exosomes and microvesicles, are nanoscale lipid bilayer particles secreted by most cell types. They carry proteins, nucleic acids, and lipids that mediate intercellular communication. Over the past decade, EVs have attracted significant attention as next-generation biologics, offering unique potential for cell-free therapies in oncology, immunomodulation, and regenerative medicine. Mesenchymal stromal cell (MSC) -derived EVs, in particular, combine regenerative potency with a favorable safety profile—avoiding the risks of cell engraftment, tumorigenicity, or undesired differentiation inherent to cell therapies.

Bottlenecks in EV manufacturing

While the therapeutic promise of EVs is clear, scalable and reproducible manufacturing remains a central challenge. Key bottlenecks include:

- Low concentration and high complexity of EV harvests in cell-conditioned media
- Co-purification of impurities such as protein aggregates, lipoproteins, and nucleic acids
- Heterogeneity of vesicle populations and lack of standardized purification methods
- Shear sensitivity of EVs during ultrafiltration or high-pressure chromatography
- Non-scalable unit operations such as ultracentrifugation and density gradients

To enable industrialization, purification workflows must provide high selectivity, minimal shear stress, consistent product quality, and linear scalability.

Membrane chromatography as a solution

Membrane chromatography offers several intrinsic advantages over traditional bead resins: convective flow transport, low diffusion resistance, and high flow rates even at large scales. The Sartobind Convec® D membrane combines a large pore structure (~1.1 µm) with polymeric ion-exchange (IEX) chemistry that enables high binding capacity for EVs and viral vectors while maintaining low shear and short residence times. Unlike resin columns, Sartobind Convec® D operates efficiently at high flow rates (residence times as low as 1–2 s), enabling rapid capture and elution of large biomolecular assemblies such as EVs. Its disposable format and modular scalability (1 mL–4.8 L) make it ideally suited for process development and GMP production.

Objective

This application note illustrates how Sartobind Convec® D can be implemented as the anion-exchange (AEX) chromatography step in a scalable EV purification process, validated through orthogonal analytics.

Materials and Methods

Upstream and harvest preparation

Human bone marrow–derived MSCs were expanded on microcarriers in a 10 L single-use bioreactor (Univessel® SU 10 L, Sartorius) under xeno-free conditions. Conditioned medium was harvested after 48 h of EV production, clarified through sequential 5 µm and 0.65 µm Sartopure® PP3 (Sartorius) filtration, and treated with Benzonase® (50 U/mL) to reduce nucleic acid content.

Tangential flow filtration 1

The downstream process is shown in Figure 1. Clarified supernatants were buffer-exchanged using Sartocon® Slice ECO-Screen Hydrosart® cassettes (300 kDa MWCO, Sartorius) on a Sartoflow® Smart tangential flow filtration (TFF) system (Sartorius). Six diavolumes were applied to remove soluble proteins and media components, yielding the EV feed for chromatography.

IEX chromatography using Sartobind Convec® D

AEX membrane chromatography was performed using Sartobind Convec® D nano (3 mL) and mini (20 mL) modules for scale-up studies.

Table 1: Buffer composition and protocol for anion-exchange chromatographic purification of MSC-derived EVs using Sartobind Convec® D

Parameter	Condition
Buffer A	20 mM Tris-HCl, pH 7.4
Buffer B	20 mM Tris-HCl, 1 M NaCl, pH 7.4
Equilibration	20 CV Buffer A
Load	Feed diluted 1:1.5 in Buffer A to ~7 mS/cm
Wash	20 CV Buffer A
Elution	Stepwise (0.2 and 0.4 M NaCl) or linear gradient (0 – 1 M NaCl)
Flow rate	9 – 20 mL/min (3 – 10 CV/min))

Analytical characterization

Orthogonal analytical tools were used to ensure EV recovery, purity, and integrity (Table 2).

Table 2: Analytical methods and respective quality attributes

Method	Quality attribute
Nanoparticle tracking analysis in fluorescence and scattering mode (NanoSight® NS300; Malvern)	Particle size and concentration
Fluorescence-based flow cytometry (Virus Counter® 3100; Sartorius)	Particle concentration
Analytical SEC-MALS (PATfix®; Sartorius)	Impurity detection
Western blot (Simple Western™; ProteinSimple)	EV identity: marker proteins (CD81, CD73, and syntenin-1)
Cryo-transmission electron microscopy	EV morphology
BCA assay	Residual protein quantification
PicoGreen™ assay (Thermo Fisher Scientific)	Residual DNA quantification
Scratch wound healing assay (Incucyte® Live-Cell Analysis System; Sartorius)	Functional assay for biological potency

Figure 1: Downstream purification process for MSC-derived EVs

Results and Discussion

Development and optimization of the Sartobind Convec® D purification strategy

Initial chromatographic screening with linear gradient elution
To establish optimal elution conditions for MSC-derived EVs on Sartobind Convec® D, we performed initial chromatography runs using a linear salt gradient from 0 to 1 M NaCl over 80 mL. The chromatography system was equipped with real-time multi-angle light scattering (RT-MALS) and dual-wavelength UV detection (260 nm and 280 nm) to enable simultaneous monitoring of particle elution and protein content.

The linear gradient screening revealed a chromatographically significant finding: two distinct populations eluted from the Sartobind Convec® D column, both at salt concentrations below 400 mM NaCl (Figure 2A). RT-MALS detection showed two partially overlapping peaks with comparable signal intensities, suggesting similar particle concentrations in both populations. However, inline UV absorbance measurements revealed a striking compositional difference. The first peak exhibited strong absorbance at 280 nm and 800 mAU at 260 nm, while the second peak demonstrated minimal UV signal below 40 mAU at 280 nm.

This chromatographic behavior indicated the presence of two populations with similar light scattering properties but markedly different protein content or composition. The mild elution conditions, with both populations eluting below 400 mM NaCl, confirmed that the AEX chemistry of Sartobind Convec® D provides sufficiently gentle binding interactions suitable for sensitive biological nanoparticles. The discrepancy between UV absorbance at 280 nm and 260 nm in the first peak suggested the presence of proteins with high aromatic amino acid content, particularly tryptophan and tyrosine, which contribute significantly to UV absorbance at these wavelengths.

Figure 2: Development of the Sartobind Convec® D elution strategy for the purification of MSC-derived extracellular vesicles. **(A)** Linear gradient elution (0 – 1 M NaCl) showing two partially overlapping peaks by RT-MALS with distinct UV absorbance profiles. **(B)** Optimized stepwise elution achieving baseline resolution at 200 mM and 400 mM NaCl.

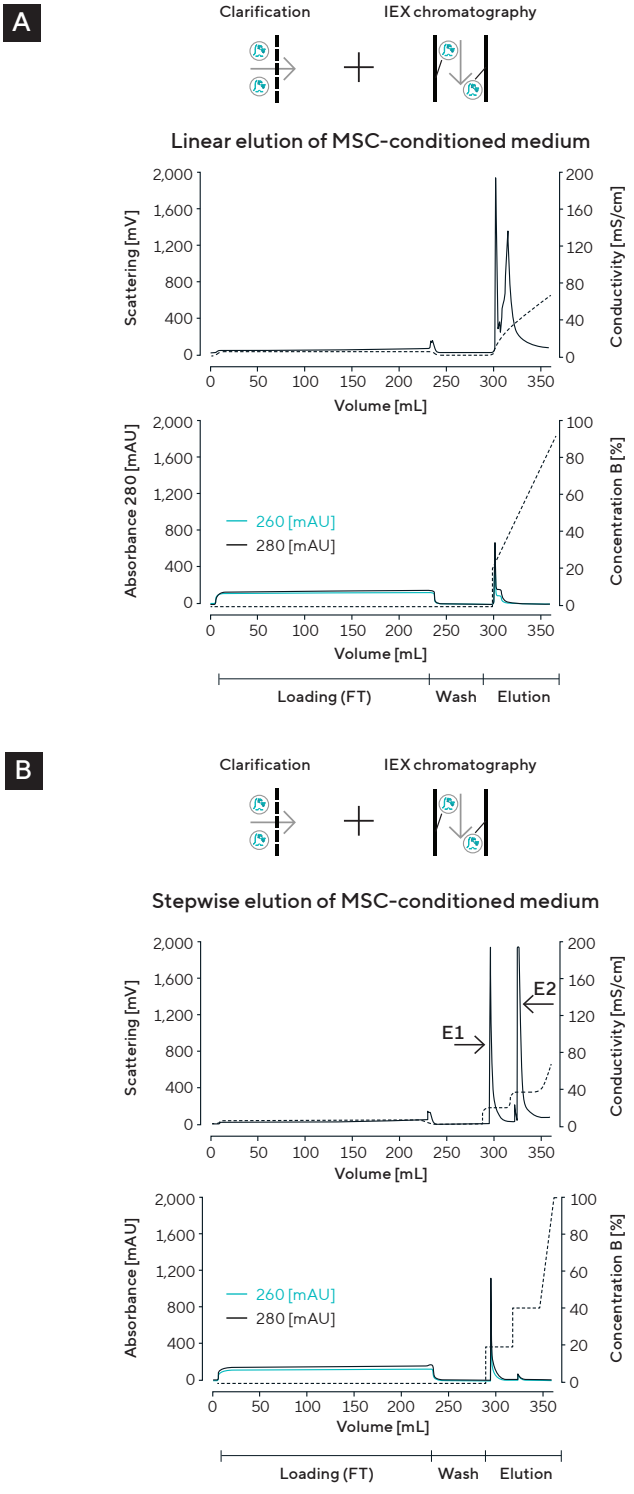

Note. E1 = elution peak 1, E2 = elution peak 2

Implementation of stepwise elution for enhanced resolution
To achieve baseline separation and enable discrete collection of these populations for detailed characterization, we transitioned from linear gradient to stepwise elution. Based on the gradient data, two discrete salt concentrations were selected: 200 mM and 400 mM NaCl. The optimized protocol included the following steps:

1. **Elution step 1:** 10 mL at 20% Buffer B (200 mM NaCl) at 3 mL/min
2. **Wash 1:** 20 mL at 20% Buffer B (minimize carryover)
3. **Elution step 2:** 10 mL at 40% Buffer B (400 mM NaCl) at 3 mL/min
4. **Wash 2:** 20 mL at 40% Buffer B
5. **Linear gradient:** 40 – 100% Buffer B (clear any remaining bound material)
6. **Strip:** 100% Buffer B (column regeneration)

This stepwise approach achieved complete baseline resolution between the two populations (Figure 2B). RT-MALS detection showed two clearly separated peaks with comparable intensities, while UV monitoring confirmed the substantial difference in protein content. Eluate 1 collected at 200 mM showed high absorbance, whereas Eluate 2 collected at 400 mM showed minimal absorbance. The intermediate wash steps proved critical for preventing cross-contamination between fractions. The 20 mL wash volumes, equivalent to approximately two column volumes for the nano format, effectively returned the baseline signal to zero. This ensured fraction purity and prevented carryover between the first and second eluates.

Process control: verification of cell-secreted origin
A critical process development question emerged: could either population originate from medium components rather than cellular secretion? To address this, unconditioned medium (medium-only control) was processed through identical workflow steps. When clarified medium alone was loaded directly onto Sartobind Convec® D without TFF pre-treatment, both RT-MALS and UV signals appeared in the 200 mM elution window (Figure 3A). No signal was detected at 400 mM. This indicated that the culture medium contained anionic components capable of binding to the AEX membrane and co-eluting with the first population.

To remove these medium-associated components, we incorporated TFF with 6× diafiltration using PBS prior to IEX chromatography. When clarified medium alone was subjected to this TFF step, then loaded on Sartobind Convec® D, no detectable RT-MALS signal appeared at either 200 mM or 400 mM, and no UV absorbance signal was observed at either elution step (Figure 3B). All signals were reduced below instrument detection limits. In contrast, when the same workflow comprising clarification, TFF, and IEX was applied to MSC-conditioned medium, both peaks remained present with excellent resolution (Figure 3C). RT-MALS intensities remained at approximately 2 V for both eluates, and the UV profile was unchanged with high absorbance for Eluate 1 and minimal absorbance for Eluate 2.

These control experiments demonstrated several key findings. First, culture medium contains anionic components that bind to Sartobind Convec® D and co-elute with non-EV particles. Second, TFF effectively removes these medium-associated impurities through diafiltration. Third, both populations detected in MSC-conditioned medium are cell-secreted rather than medium-derived. Fourth, the TFF step is essential for achieving high-purity EV preparations and must be integrated upstream of IEX chromatography.

Figure 3: Process control experiments demonstrating cell-secreted origin of both populations. **(A)** Medium-only control before TFF showing signal at 200 mM. **(B)** Medium-only control after TFF showing complete signal elimination. **(C)** MSC-conditioned medium after TFF maintaining both peaks, confirming cell-secreted origin.

A Medium-only control — stepwise elution

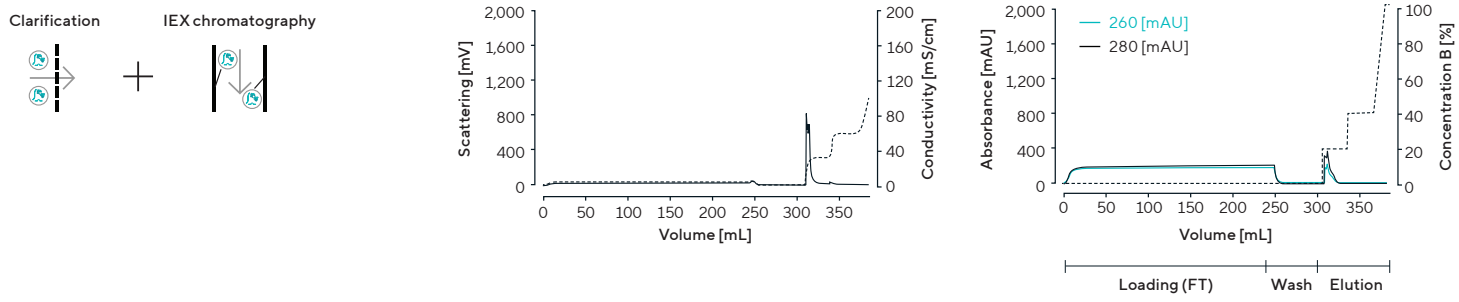

B Medium-only control — TFF + stepwise elution

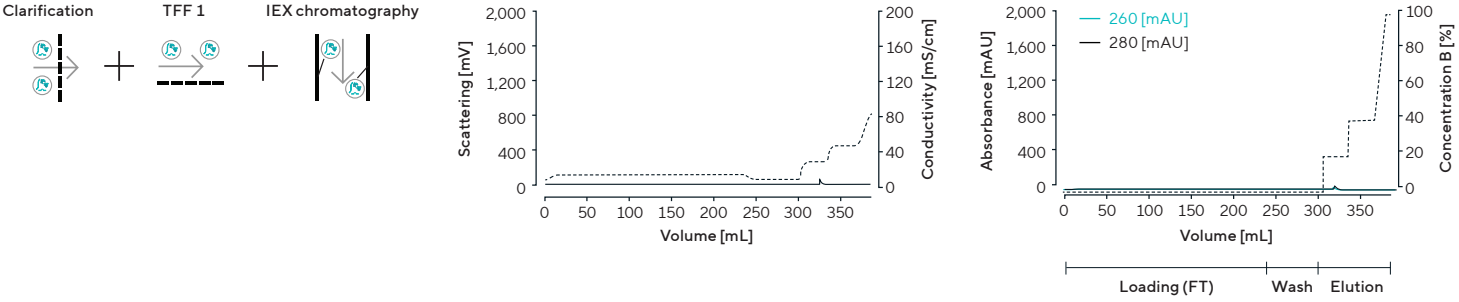

C MSC-conditioned medium — TFF + stepwise elution

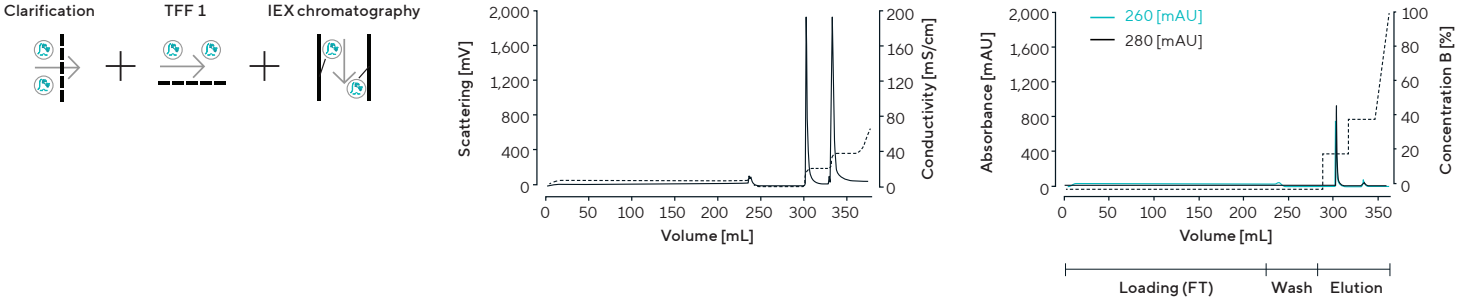

Process reproducibility and binding performance

Independent run validation

To establish a robust process, three independent downstream processing runs were performed starting from different 100 mL aliquots of MSC-conditioned medium from the same bioreactor harvest. Each run followed the complete workflow: clarification, nuclease treatment, TFF with 6× diafiltration, and IEX on Sartobind Convec® D. Across all runs, highly consistent elution profiles were obtained on both RT-MALS and UV detectors (Figure 4), demonstrating excellent process reproducibility.

Column performance and binding capacity

To evaluate the capture efficiency of Sartobind Convec® D, the flow-through from the loading step was collected and re-injected onto a fresh column. The RT-MALS signal in the flow-through was below 0.1 V, representing background level, and UV signal in the flow-through rerun showed no detectable peaks at either elution step (Figure 5). The absence of detectable signal upon flow-through rerun confirmed near-quantitative binding efficiency during the initial loading of MSC-conditioned medium. This indicates that the membrane capacity was not exceeded and that binding kinetics were fast enough to capture particles even at the high flow rates used.

Figure 4: Reproducibility of the complete MSC-EV downstream processing workflow assessed across three independent runs **(A–C)**

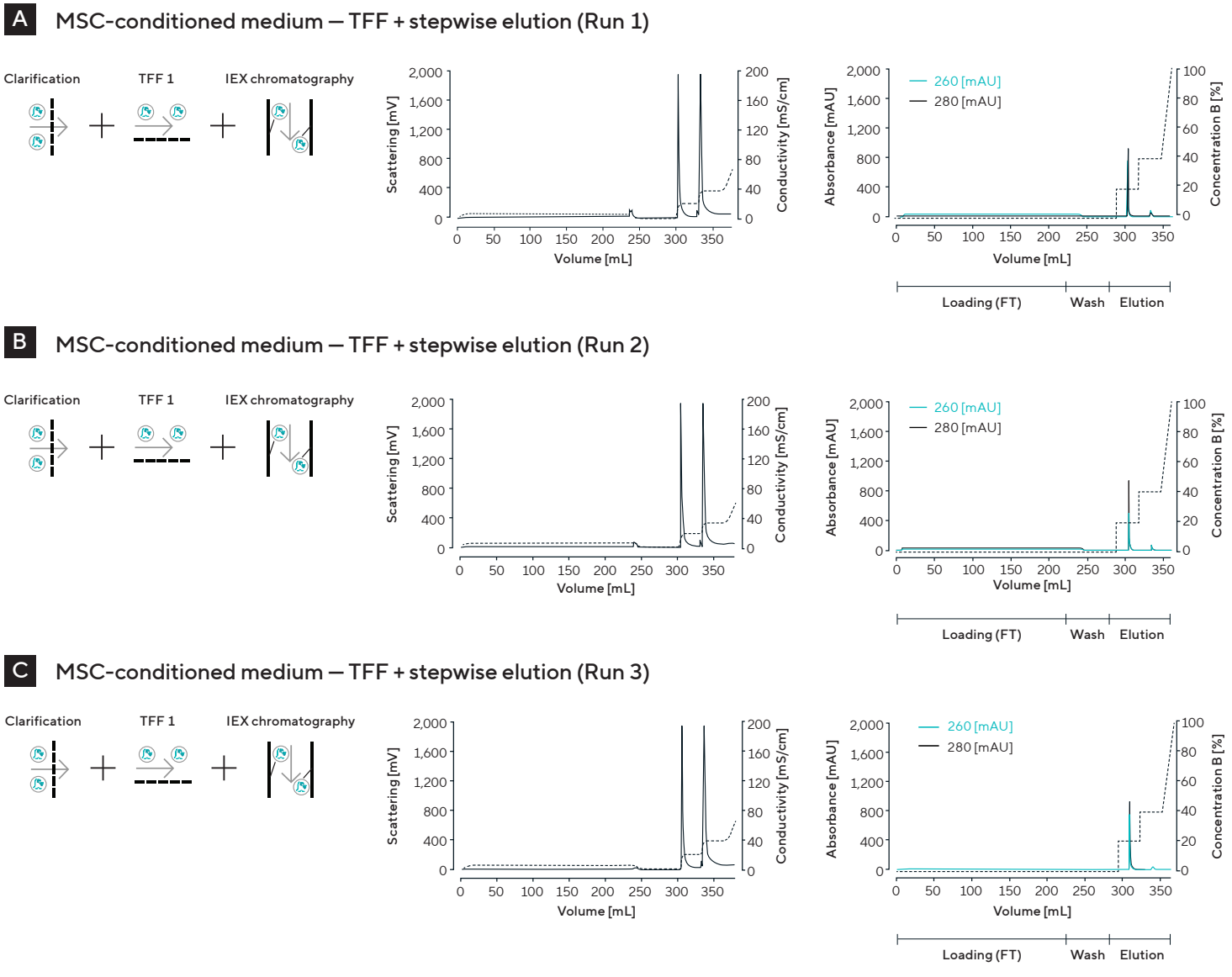

Figure 5: Binding efficiency verification through flow-through reloading. Flow-through samples were re-injected onto fresh columns with TFF pre-treatment (Run 1 shown here).

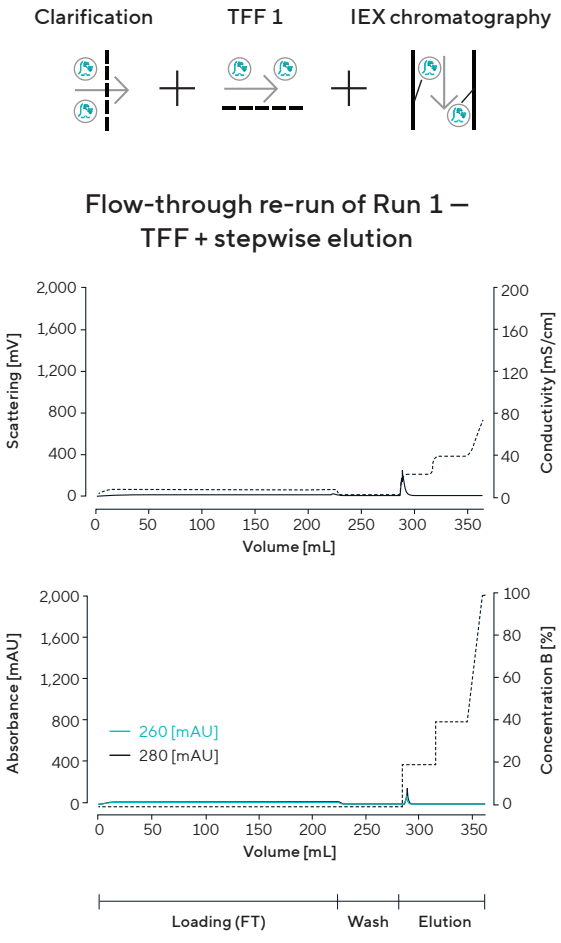

For the nano format with 3 mL bed volume, 250 mL of diluted sample consisting of 100 mL MSC-conditioned medium plus 150 mL Buffer A was successfully loaded without any breakthrough or capacity limitation. This represents a sample-to-column volume ratio exceeding 83:1, demonstrating the exceptionally high binding capacity of the membrane adsorber format relative to traditional packed-bed resins. The high capacity can be attributed to the open, homogeneous pore structure with an average pore size of approximately 1.1 µm, offering an adequate balance between high permeability over large process volumes and a large inner membrane surface accessible to particles of EV size. Additionally, the convective flow through the membrane pores, rather than diffusive transport into resin beads, ensures rapid mass transfer even at high flow rates.

Comprehensive characterization of Sartobind Convec® D eluates

RT-MALS detection: a critical analytical tool

RT-MALS detection proved essential for identifying and optimizing the separation of the two populations. Relying solely on UV absorbance would have resulted in collection of only Eluate 1, the high-protein fraction, while missing Eluate 2 (Figure 2B). This highlights a critical consideration: the EV-enriched fraction exhibited minimal UV absorbance, rendering it essentially invisible to conventional chromatography UV detection. This phenomenon occurs because intact vesicles contain relatively little protein per particle compared to the light they scatter, and the lipid bilayer itself does not significantly absorb UV light at 280 nm. This underscores the importance of orthogonal detection methods — particularly light scattering — for EV process development and monitoring. Without MALS capability, manufacturers relying on standard chromatography systems with UV detection alone would likely discard the EV-enriched fraction as non-product, resulting in complete product loss.

Orthogonal particle quantification across analytical platforms

Single-particle analysis techniques revealed important differences between the two eluates that provided insights into their fundamental compositional nature (Figure 6). When quantified by scattering-based nanoparticle tracking analysis (Sc-NTA), both eluates showed similar particle concentrations (both 2×10^{10} particles/mL), consistent with the RT-MALS data obtained during chromatography (both 2 V). This convergence between two independent methods validated the initial observation that both populations contained comparable numbers of particles with similar scattering cross-sections.

However, fluorescence-based methods following optimized CellMask™ Orange (Invitrogen) labeling revealed a striking divergence. CellMask™ Orange is a lipophilic dye that intercalates into lipid bilayer membranes, labeling intact vesicles while remaining largely unassociated with non-membranous particles. For Eluate 2, all three quantification techniques converged on similar particle concentrations, with Sc-NTA, fluorescence NTA (Fl-NTA), and fluorescence flow cytometry (Fl-FC) yielding comparable values.

This convergence strongly suggested that Eluate 2 consisted predominantly of membrane-enveloped vesicles capable of incorporating the lipophilic fluorescent dye.

In stark contrast, for Eluate 1, fluorescence-based methods detected only approximately 15 – 27% of particles counted by scattering-based techniques. This dramatic divergence suggested that Eluate 1 predominantly contained non-membranous particles that scatter light, but do not efficiently incorporate lipophilic fluorescent dyes. These particles likely represent protein aggregates, lipoproteins, or other non-vesicular extracellular particles that possess sufficient size and refractive index contrast to scatter light but lack the organized lipid bilayer structure required for dye intercalation.

Quantitative analysis of the eluates relative to the IEX load revealed that both Eluate 1 and Eluate 2 recovered 24% of particles when quantified by Sc-NTA, suggesting similar binding and elution efficiencies for light-scattering particles regardless of their molecular composition. However, when using FI-NTA, only 5% of particles were recovered in Eluate 1 compared to 28% in Eluate 2. This pattern was independently confirmed by FI-FC, which detected 4% of particles in Eluate 1 and 31% in Eluate 2 (Figure 7 and Table 3).

The close agreement between FI-NTA and FI-FC measurements, both fluorescence-based but mechanistically distinct techniques, strengthened confidence in the conclusion that Eluate 2 represents an authentic EV-enriched fraction while Eluate 1 contains predominantly non-vesicular material.

Figure 7 summarizes the key performance metrics of the Sartobind Convec® D step, including particle recovery, total protein removal, and residual DNA reduction compared to the TFF retentate. In Eluate 2, representing the EV-enriched fraction, protein concentration decreased by more than 99.5% after Convec® D purification, as determined by BCA assay. Double-stranded DNA, measured by PicoGreen™ assay, decreased by over 95.5%, demonstrating effective clearance of both proteinaceous and nucleic acid contaminants while maintaining high recovery of membranous vesicles.

Figure 6: Orthogonal particle quantification revealing compositional differences between eluates. Comparison of Sc-NTA, FI-NTA, and FI-FC measurements shows method convergence for Eluate 2 but divergence for Eluate 1, indicating membranous and non-membranous particle populations.

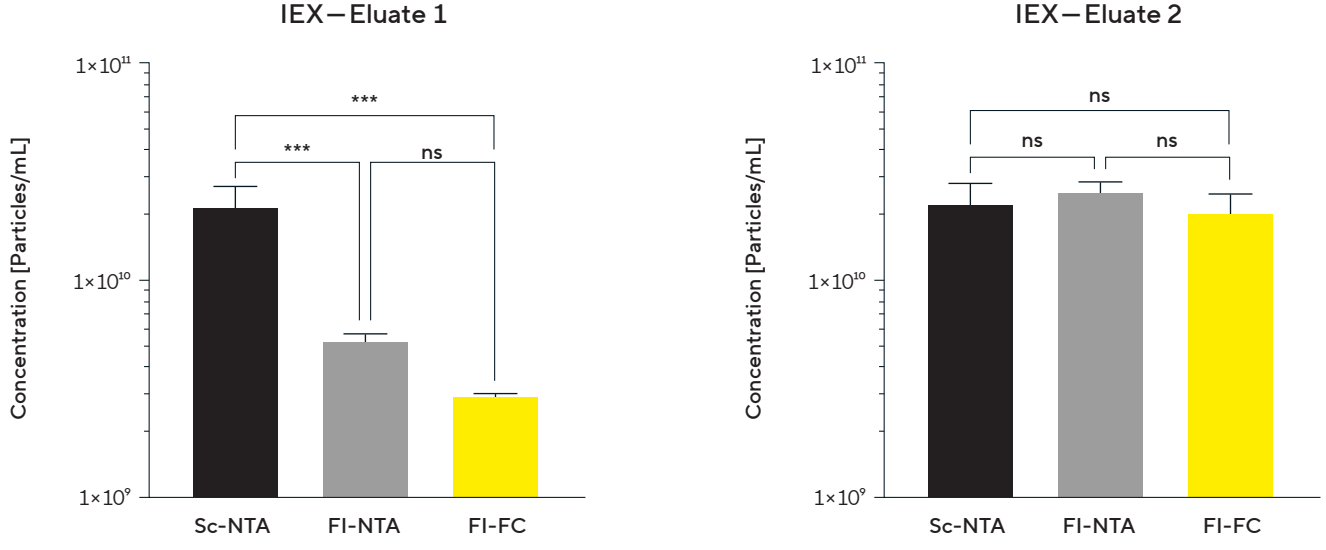

Figure 7: IEX step evaluation by orthogonal analytics. **(A – C)** Particle recovery quantified by Sc-NTA, FI-NTA, and FI-FC. **(D – F)** Impurity removal assessed by BCA assay, analytical SEC-MALS-UV-Fluorescence, and PicoGreen™ assay

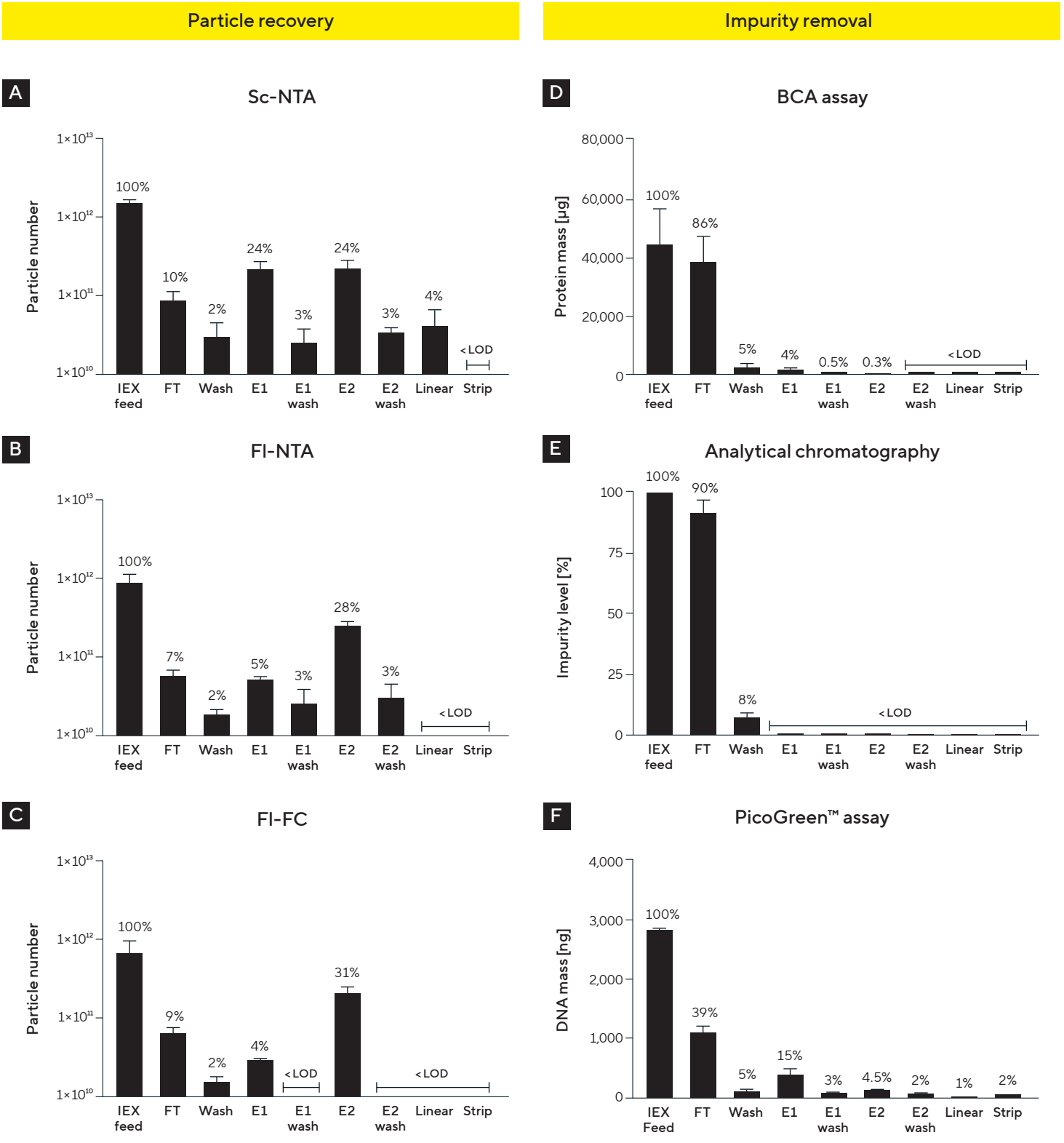

Morphological characterization by transmission electron microscopy

Cryo-transmission electron microscopy (cryo-TEM) provided definitive visual evidence of the compositional differences between eluates, confirming the chromatographic and analytical data at the ultrastructural level (Figure 8). Eluate 2, collected at 400 mM NaCl and representing the EV-enriched fraction, displayed abundant vesicular structures throughout the field of view. These structures exhibited the characteristic cup-shaped morphology typical of negatively stained EVs, a result of the collapse of spherical vesicles onto the cryo-TEM grid during sample preparation and drying. Intact lipid bilayer membranes were clearly visible as darker electron-dense rings surrounding lighter interiors.

The size range spanned from 50 to 200 nm in diameter, consistent with the expected dimensions for small extracellular vesicles according to MISEV2023 classification.[1] The population appeared homogeneous with minimal background debris, and the estimated purity based on visual inspection exceeded 90% vesicular structures.

In striking contrast, Eluate 1, collected at 200 mM NaCl and representing the non-vesicular extracellular particle (NVEP)-enriched fraction, displayed predominantly electron-dense amorphous material lacking the cup-shaped morphology characteristic of EVs. No clear membranous structures were visible in the majority of the fields of view.

Figure 8: Cryo-TEM of chromatographic fractions. TEM images of the **(A)** first (200 mM) and **(B)** second (400 mM) eluates showing vesicle-rich morphology in Eluate 2 versus non-vesicular, protein-rich appearance in Eluate 1. Scale bars = 500 nm

A

Elution 1

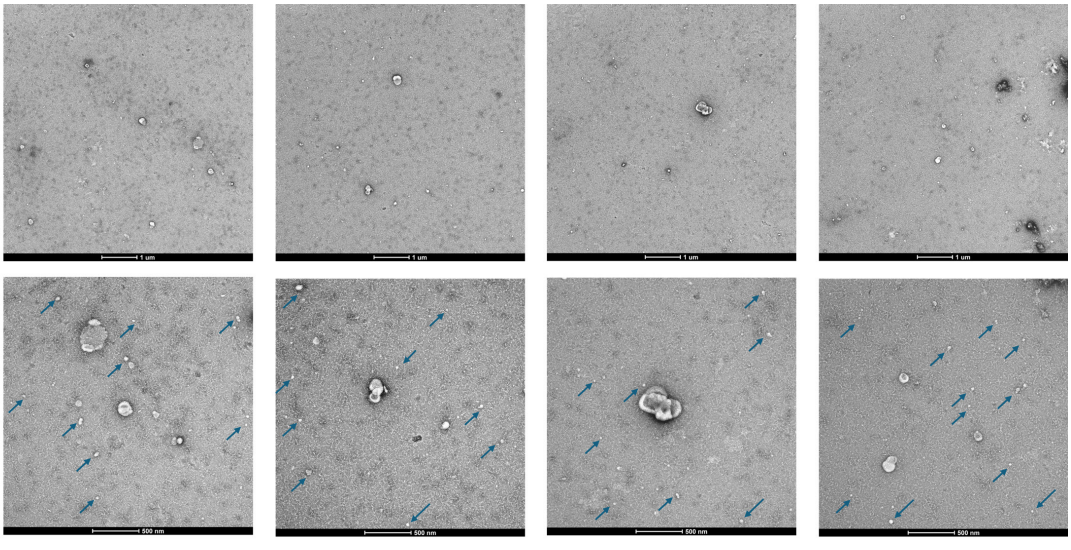

B

Elution 2

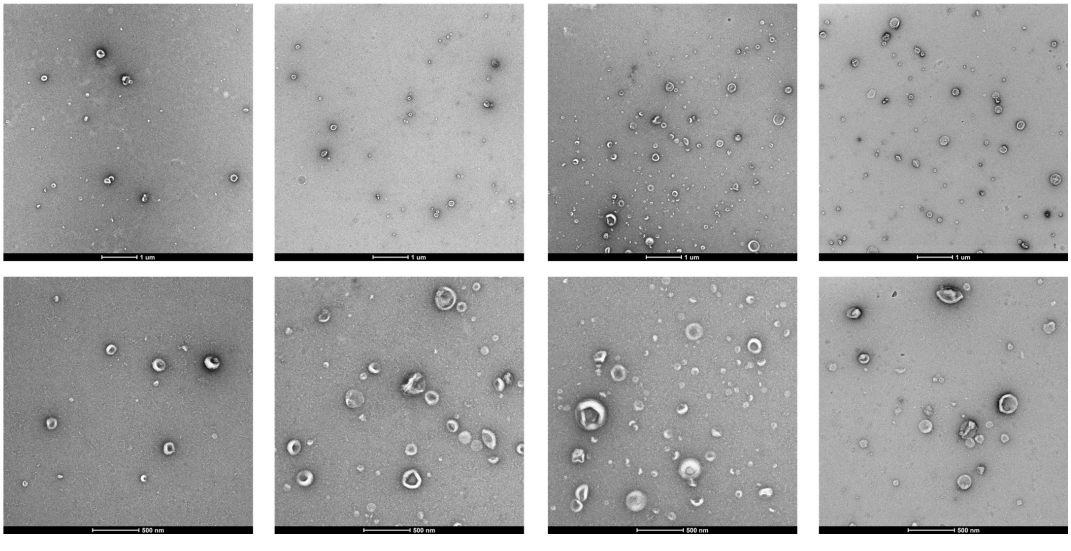

Instead, the appearance was heterogeneous with protein aggregates and irregular fragments. Occasional vesicular structures were present, estimated at less than 10% of total material, likely representing co-eluted EVs that bound less strongly to the membrane. Heavy background staining indicated high protein content, consistent with the strong UV absorbance observed during chromatography.

These ultrastructural images conclusively demonstrated that Sartobind Convec® D effectively separated membranous extracellular vesicles in Eluate 2 from non-vesicular extracellular particles in Eluate 1. These represent two populations that were indistinguishable by conventional light scattering methods alone but fundamentally different in structure and composition when examined by orthogonal techniques.

Size distribution analysis by dynamic light scattering

Dynamic light scattering measurements revealed clear size differences between the two populations that correlated with their structural differences observed by cryo-TEM. Eluate 1 displayed a mean hydrodynamic diameter of 22 nm with a modal value of 18 nm (Figure 9). The small size of these particles, in the range of 20 to 30 nm, is consistent with reported dimensions of exomeres and other small non-vesicular extracellular particles described in recent literature.[2] These particles likely represent protein complexes, small lipoproteins, or protein-nucleic acid aggregates that elute early from the AEX membrane due to lower surface charge density.

Eluate 2 displayed a mean hydrodynamic diameter of 115 nm with a modal value of 89 nm. This size distribution falls within the expected range for small extracellular vesicles according to MISEV2023 guidelines, which define small EVs as particles with diameters between 50 and 200 nm.[1] The larger hydrodynamic diameter compared to Eluate 1 is consistent with the presence of intact lipid bilayer vesicles, which scatter light more intensely and occupy greater hydrodynamic volume than compact protein aggregates of similar mass.

Figure 9: Size distribution by dynamic light scattering. Analysis showing size distribution profiles of **(A)** Eluate 1 and **(B)** Eluate 2. Data represent mean ± SD, n = 3

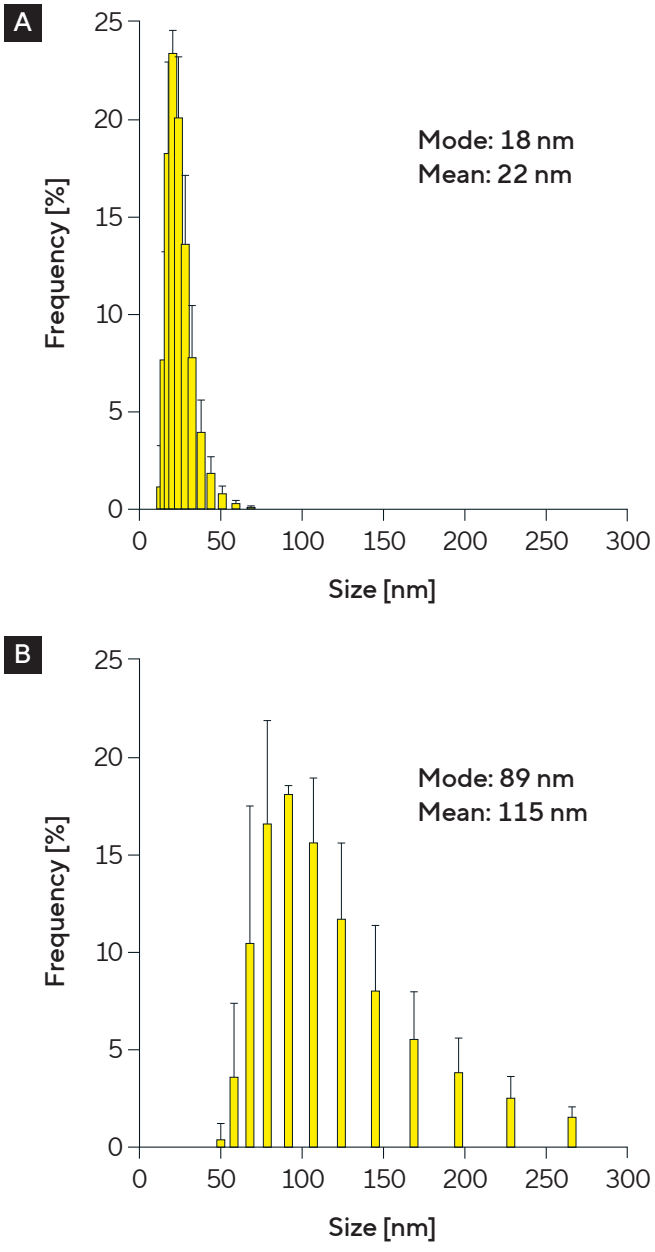

Analytical size-exclusion chromatography for purity assessment

Multi-detector analytical size-exclusion chromatography (SEC) incorporating MALS, UV absorbance, and intrinsic fluorescence detection provided comprehensive purity assessment across all process streams. This technique separates particles and molecules by size while simultaneously measuring their concentration through multiple independent detection modes, enabling differentiation between EVs and various impurity classes.

Protein quantification by BCA assay showed that 86% of the feed protein was present in the flow-through (Figure 7D), indicating that the majority of soluble proteins did not bind to the Sartobind Convec® D membrane under the loading conditions employed. This was consistent with analytical chromatography area under the curve analysis, which indicated that 90% of impurities, detected by UV absorbance and eluting in the 14 – 20-minute retention time region, remained in the flow-through (Figure 10A and B). Chromatographic profiles of the flow-through confirmed the presence of the impurity peak, highlighted in green in the 14 – 20-minute window, and complete absence of signal in the EV size fraction, highlighted in red in the 9 – 14-minute window. This confirmed efficient capture of larger particles such as EVs on the column while allowing smaller soluble proteins to pass through unbound.

A small UV absorbance and intrinsic fluorescence signal was observed in the impurity elution window during the wash step, representing the 14 – 20-minute retention time region. This indicated residual impurity clearance during the wash phase (Figure 10 C), with weakly bound or non-specifically associated proteins being removed before the targeted elution steps. This wash step therefore contributed to the final product purity by removing the last traces of contaminating proteins that might otherwise co-elute with the product.

Eluate 2, representing the high-purity EV fraction, displayed a strong MALS signal in the void volume between 9 and 13 minutes, corresponding to particles in the EV size range that are too large to enter the pores of the SEC column and therefore elute earliest (Figure 10 F). Critically, this fraction showed minimal UV absorbance in the protein region between 14 and 20 minutes and no detectable fluorescence signal in the small molecule region between 20 and 30 minutes. This profile is characteristic of purified vesicle preparations with low protein and nucleic acid contamination.

Eluate 1, representing the NVEP fraction, displayed a strong MALS signal in the void volume similar to Eluate 2, confirming that both fractions contained light-scattering particles of similar size by SEC (Figure 10 D). However, Eluate 1 exhibited a prominent UV absorbance peak at 9 – 13 minutes — corresponding to protein impurities — as well as additional fluorescence signals corresponding to smaller contaminants such as free nucleic acids or small molecules, which was not observed for Eluate 2. This multi-peak profile indicated a heterogeneous mixture of particle types and molecular species in the NVEP fraction.

The analytical SEC data quantitatively confirmed what cryo-TEM showed qualitatively: the stepwise elution strategy with Sartobind Convec® D successfully separated high-purity EVs in Eluate 2 from a mixed NVEP and impurity population in Eluate 1. The strong correlation between independent analytical methods, including light scattering, UV absorbance, fluorescence, and electron microscopy, provided robust evidence for the chromatographic mechanism and product identity.

Figure 10: AEX step evaluation using multi-detector analytical chromatography. SEC with inline MALS, UV absorbance, and intrinsic fluorescence detection was used to evaluate the distribution of particles and impurities: **(A)** load, **(B)** flow-through and **(C)** wash samples. Comparison of eluates: **(D and E)** Elution 1 and wash, **(F and G)** Elution 2 and wash, as well as **(H)** linear (in which salt concentration was increased from 400 to 1,000 mM) and **(I)** strip (in which salt concentration was kept as 1,000 mM). n = 3 independent downstream runs.

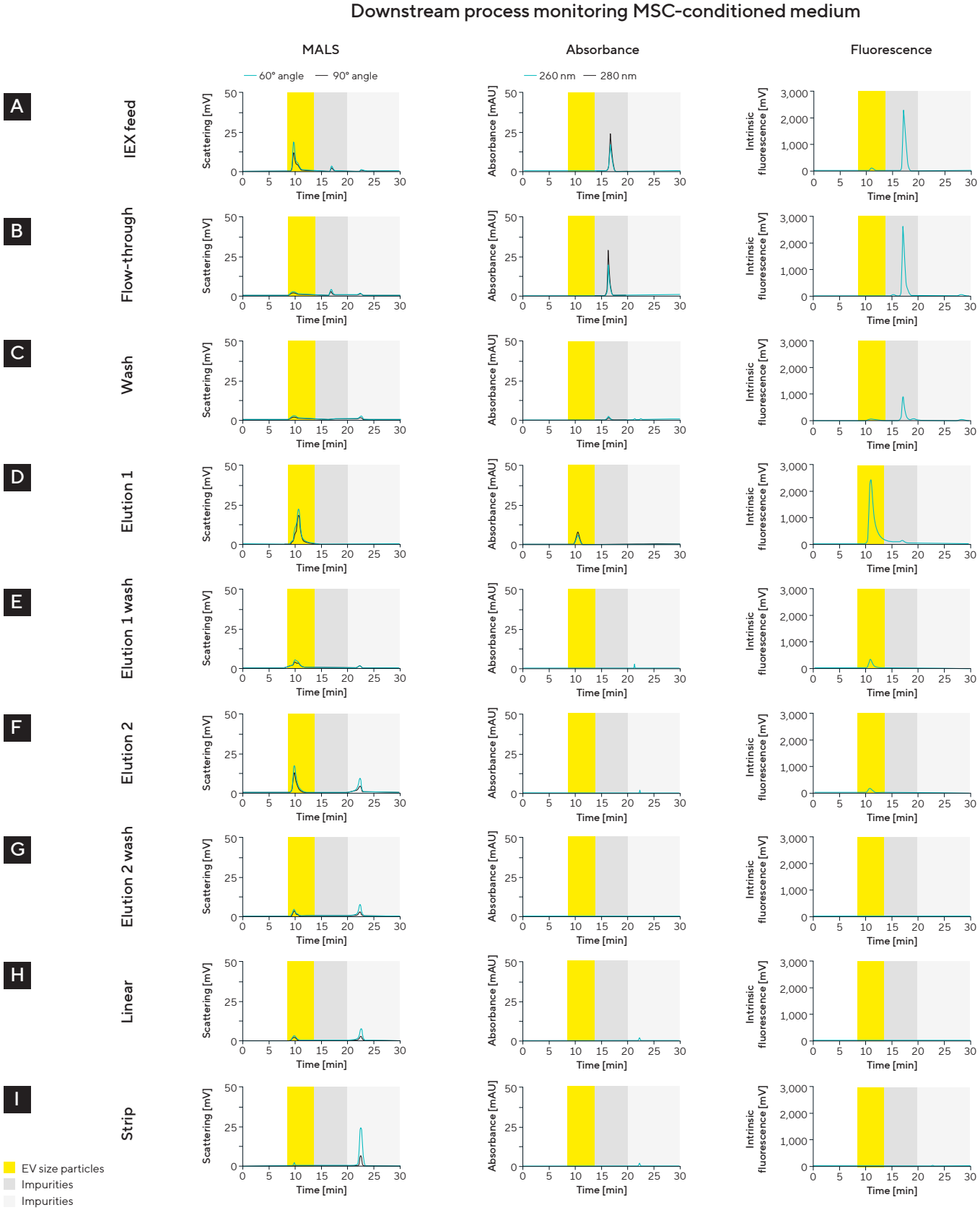

Molecular identity: EV marker analysis by Simple Western™

Capillary electrophoresis-based immunoassay using the Simple Western™ platform provided semi-quantitative expression data for key markers aligned with MISEV2023 guidelines. This technique separates proteins by size through capillary electrophoresis, then detects them using specific antibodies, providing both molecular weight confirmation and relative quantification.

Analysis of positive EV markers showed strong enrichment in Eluate 2 (Figure 11). CD81, a tetraspanin protein highly enriched in EV membranes, displayed a strong band in Eluate 2 compared to a faint band in Eluate 1. CD73, an ecto-5'-nucleotidase that serves as a MSC marker, was highly enriched in Eluate 2 and was also detected in the cell lysate, confirming MSC origin of the EVs. Syntenin-1, an EV-associated protein involved in vesicle biogenesis, was only detected in Eluate 2 and the cell lysate but not detected in Eluate 1.

Analysis of negative or contamination markers showed the opposite pattern. Albumin, a soluble serum protein that represents a common contaminant in EV preparations, was strongly enriched in Eluate 1 while being essentially absent in Eluate 2. Calnexin, an endoplasmic reticulum resident protein that serves as a marker of cellular contamination, was absent in both eluates while present in cell lysate control, confirming minimal contamination from intracellular compartments.

The marker profile demonstrated several key findings. First, Eluate 2 expresses canonical EV markers including tetraspanin CD81, as well as MSC-specific surface proteins CD73, confirming its identity as an MSC-derived EV preparation. Second, Eluate 1 is enriched in soluble protein contaminants, particularly albumin, consistent with its classification as a non-vesicular extracellular particle fraction. Third, both eluates show minimal cellular contamination based on the absence of endoplasmic reticulum markers such as calnexin, indicating that the upstream clarification and nuclease treatment steps effectively removed cellular debris. Fourth, Sartobind Convec® D successfully separated EVs from albumin and other serum proteins, addressing one of the major purification challenges in EV manufacturing.

Figure 11: EV marker expression by Simple Western™ confirming EV marker expression (CD81, CD73, and syntenin-1) and absence of negative markers (calnexin and albumin) in Eluate 2

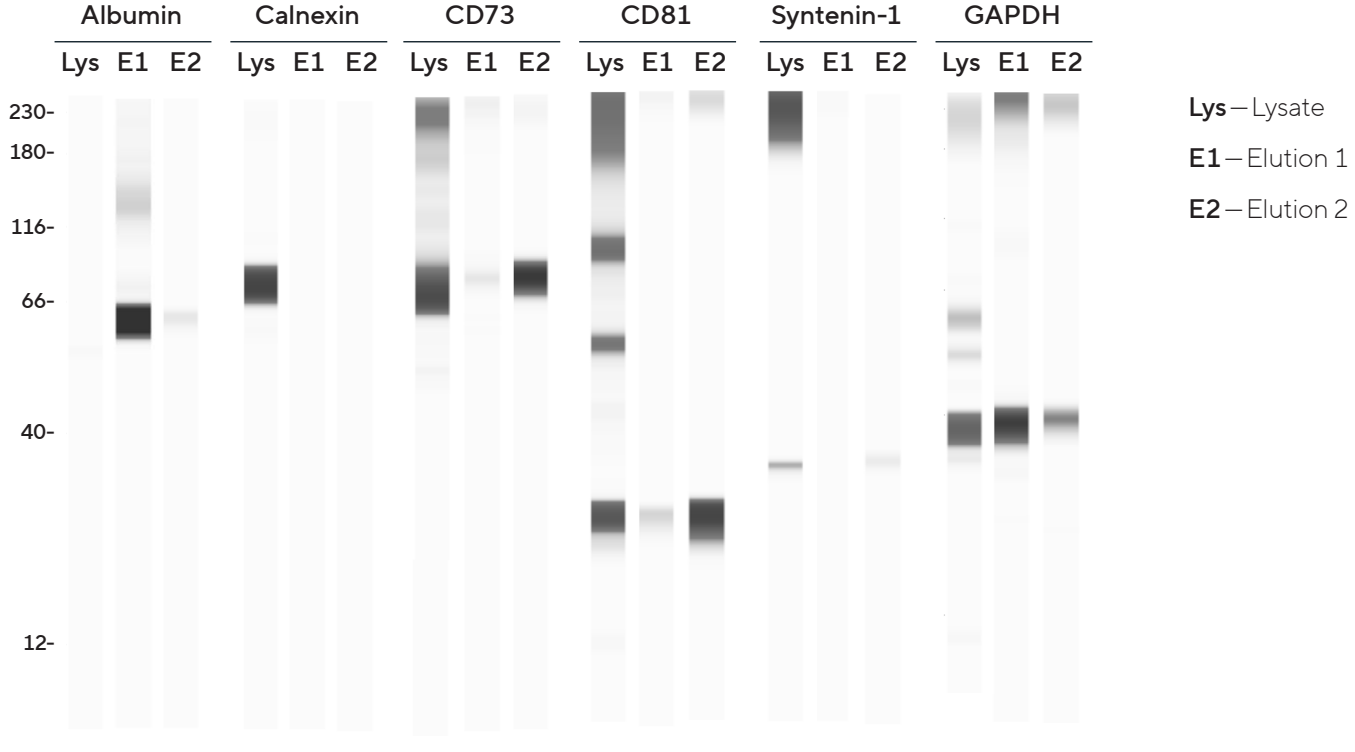

Functional validation: biological activity preservation

The functionality of purified EVs was verified in a physiologically relevant biological context through in vitro scratch wound healing assays using human dermal fibroblasts. This assay models wound closure through cell migration and proliferation, biological processes known to be stimulated by MSC-derived EVs through paracrine signaling mechanisms. Figure 12 presents results demonstrating that cells treated with EVs (at a dose of 8.5×10^4 particles/seeded fibroblast) purified through the Sartobind Convec D workflow exhibited migration and wound closure rates significantly higher than the negative control (0% FBS medium), as measured by cell density recovery within the wound area. In contrast, control cells receiving only vehicle (0% FBS medium) showed minimal closure over the same time course. EVs were stained with Incucyte® Exofluor EV Labeling Dye (Sartorius) to visualize uptake by fibroblasts using the Incucyte® Live-Cell Imaging System. Labeled EVs stimulated similar wound recovery to unlabeled EVs. Furthermore, labeled EVs were clearly taken up by fibroblasts compared with a dye-only control.

Figure 12: Human dermal fibroblasts treated with MSC-derived EVs show significant wound closure compared to 0% FBS medium, quantified by cell density recovery within the wound area, at 48 h. **(A)** Percentage wound recovery over time up to 48 h post scratch, **(B)** final wound recovery at 48 h post scratch. Statistical analysis by one-way ANOVA with Tukey's test (*p < 0.05, **p < 0.01, ***p < 0.001, ****p < 0.0001; ns not significant). **(C)** Incucyte® Exofluor EV Labeling Dye-only treatment of fibroblasts, **(D)** treatment of fibroblasts with labeled EVs

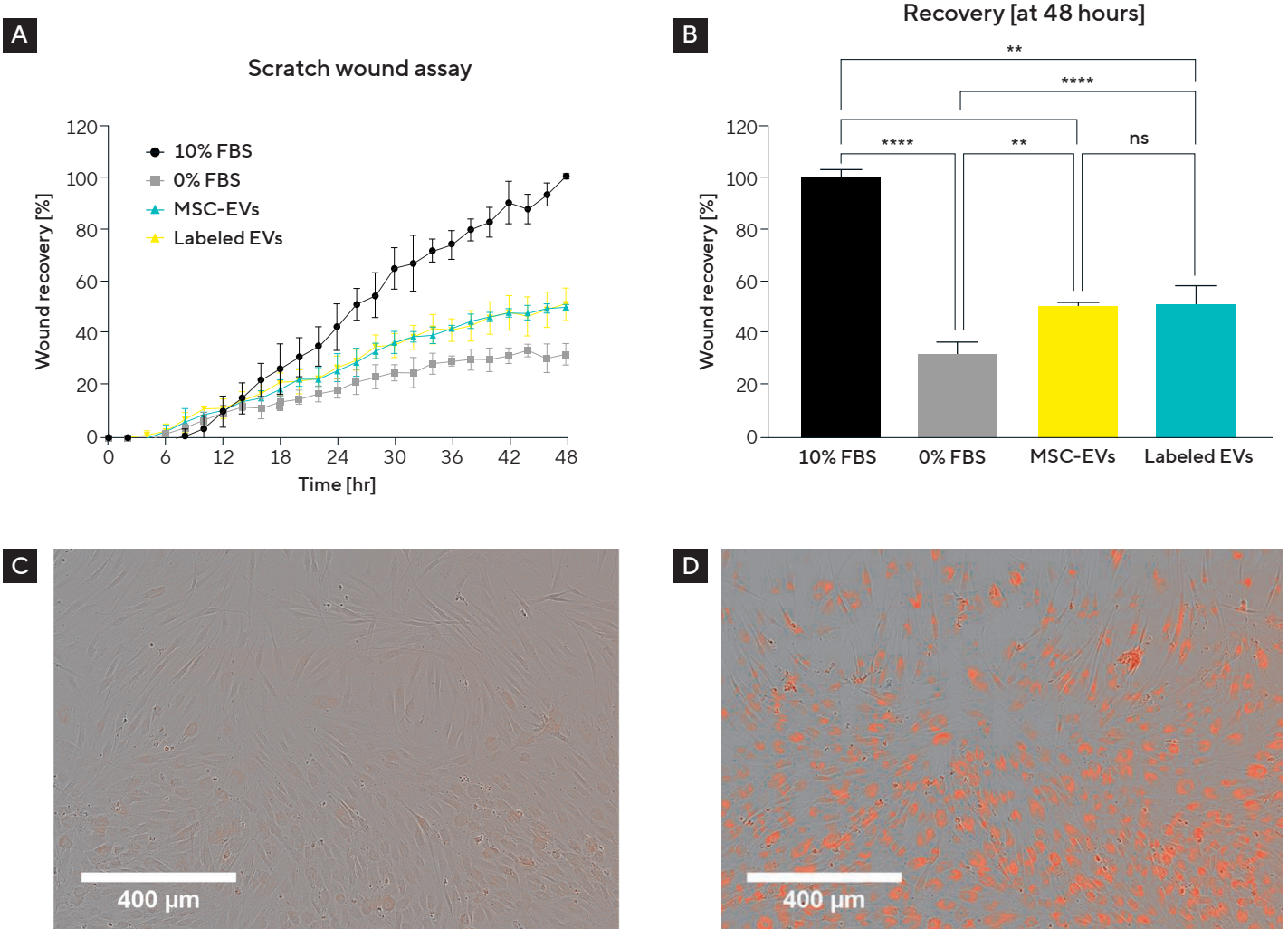

This functional validation demonstrates that the gentle convective separation mechanism of Sartobind Convec® D preserves vesicle bioactivity, a critical quality attribute for therapeutic development, while achieving substantial impurity clearance. The preservation of biological activity indicates that the surface proteins mediating cellular interactions and the internal cargo molecules responsible for therapeutic effects remain intact and functional after the purification process. This is particularly important given that alternative purification methods such as ultracentrifugation or precipitation can damage vesicles through high shear forces or chemical denaturation, potentially compromising their therapeutic potential.

This architectural feature eliminates many of the scale-dependent mass transfer limitations that complicate scale-up of traditional packed-bed chromatography.

These features confirm that the Sartobind Convec® D step can be directly transferred from laboratory to pilot- or production-scale systems with minimal re-optimization, greatly simplifying process development timelines and reducing time-to-clinic. The modular nature of the membrane format, available in sizes ranging from 3 mL to 1,200 mL, enables seamless scaling by simply increasing the membrane area while keeping all other process parameters constant.

Process scalability: linear scale-up demonstration

A critical requirement for industrial implementation is predictable process scalability that enables direct transfer of laboratory-scale methods to manufacturing scale with minimal re-optimization. To evaluate the scalability of the downstream processing workflow, feed volume was increased from 100 mL to 700 mL and each unit operation was adjusted proportionally. The same operating conditions, including flow rate per membrane volume, buffer compositions, and residence times, were applied to both 3 mL (small-scale) and 20 mL (scaled-up) Sartobind Convec® D modules.

For IEX chromatography, only the EV-containing eluate, Eluate 2, was analyzed in detail (Figure 13). Particle recoveries for this process step were 19% measured by Sc-NTA, 24% measured by FI-NTA, and approximately 39% measured by FI-FC. These values remained consistent with the small-scale runs. Analytical chromatography showed complete removal (99.8%) of the impurity peak in the 14 – 20-minute retention window, while BCA analysis indicated 98% protein removal compared to the starting material. DNA concentration was reduced to 0.3% (by 99%) of the original feed concentration, as determined by PicoGreen™ assay.

The resulting data, summarized in Table 3, demonstrate linear scalability, with particle recovery maintained as membrane volume and flow rate were scaled proportionally while residence time remained constant. The strong linear correlation between processed volume and recovered particle count highlights the predictable behavior of the convective flow membrane architecture, which relies on flow through large pores rather than diffusion into small pores.

Figure 13: Linear scalability of the MSC-EV purification process from 3 mL to 20 mL Sartobind Convec® D membrane volume. **(A)** Complete downstream processing workflow schematic and chromatography profile. **(B-D)** Particle recovery by Sc-NTA, FI-NTA, and FI-FC in final Eluate 2. **(E)** Protein removal. **(F)** Impurity clearance by analytical SEC-MALS. **(G)** DNA removal.

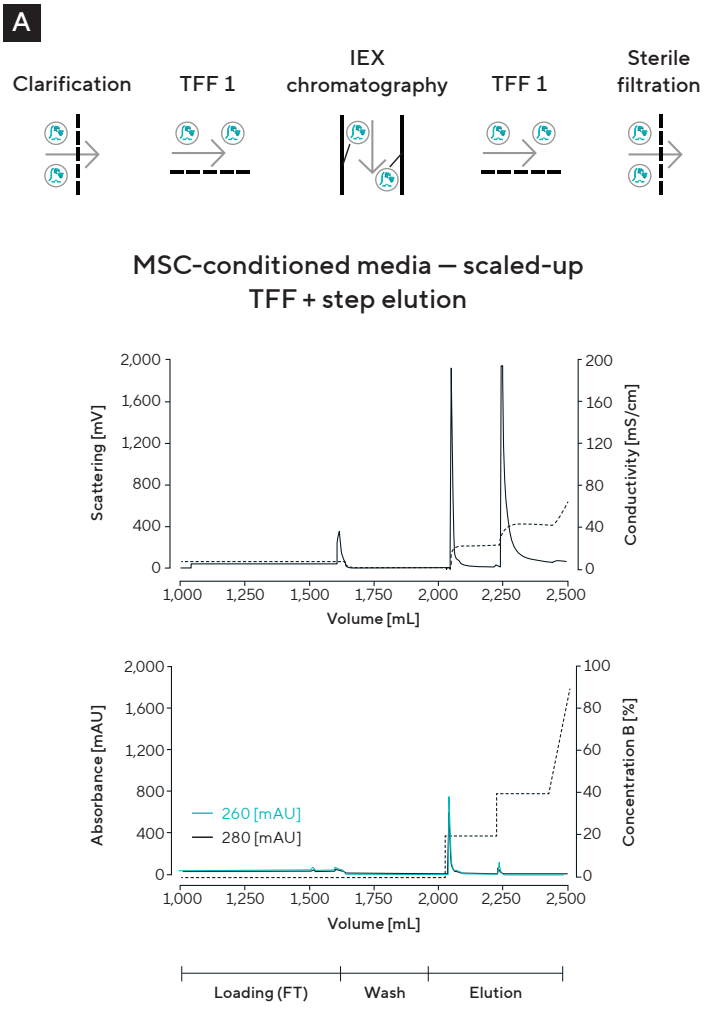

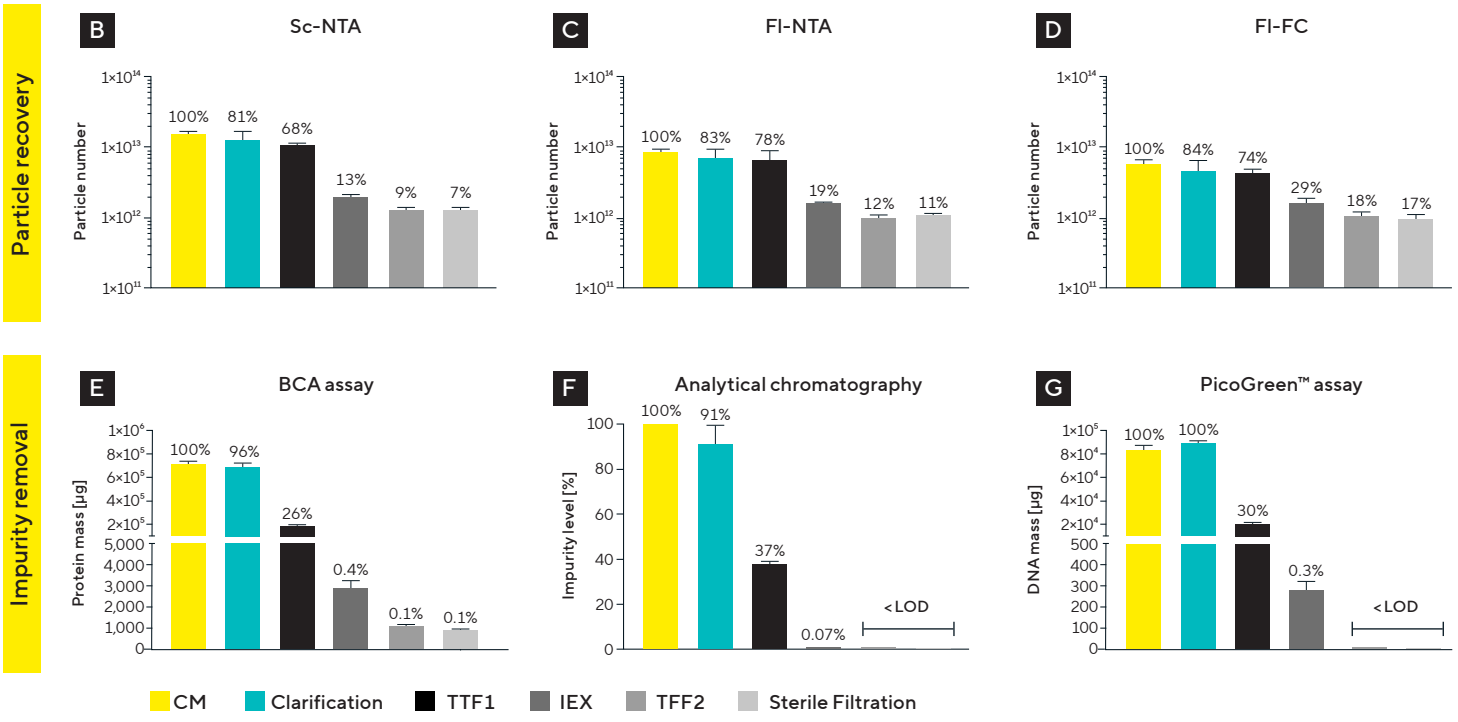

Table 3: Particle recoveries measured by Sc-NTA, FI-NTA, and FI-FC at the two IEX development process stages: small-scale end-to-end runs and a scaled-up end-to-end run.

	Technique	Eluate 1	Eluate 2
Small-scale run (n=3)	Sc-NTA	24% recovery	24% recovery
	FI-NTA	5% recovery	28% recovery
	FI-FC	4% recovery	31% recovery
Scaled-up run	Sc-NTA	N/A	19% recovery
	FI-NTA	N/A	24% recovery
	FI-FC	N/A	39% recovery

The combination of analytical, biophysical, and functional results provides comprehensive validation that Sartobind Convec® D delivers a robust, scalable, and biologically compatible purification step for EV manufacturing. These findings demonstrate that Sartobind Convec® D enables both effective impurity clearance and preservation of vesicle integrity across multiple process scales. The ability to reproducibly separate non-vesicular extracellular particles from functional EVs, coupled with high throughput operation and short process times typically under one hour per batch, positions the Sartobind Convec® D membrane as a cornerstone technology for industrial EV downstream processing.

Summary and Conclusion

This application note establishes Sartobind Convec® D membrane chromatography as an enabling technology for scalable purification of therapeutic-grade extracellular vesicles. The integration of large-pore membrane architecture, optimized weak AEX chemistry, and convective flow dynamics creates a separation environment uniquely suited to lipid-bound biological nanoparticles. The experimental data demonstrate that MSC-derived EVs can be effectively captured and purified in a single IEX step with performance metrics exceeding 99% binding efficiency, 98% total protein clearance, 99% DNA removal, and greater than 39% particle recovery while maintaining biological activity. Complete baseline resolution between vesicular and non-vesicular populations addresses the critical challenge of defining product identity with analytical rigor, establishing a clear chromatographic signature that supports compliance with MISEV2023 guidelines and emerging regulatory expectations.

The membrane's ability to preserve vesicle morphology and bioactivity while achieving substantial impurity clearance stems from its fundamental design. Unlike traditional packed-bed resins requiring residence times of several minutes and diffusive transport through tortuous pore networks, the Sartobind Convec® D membrane enables binding and desorption within seconds through direct convective flow. This minimizes shear exposure and process time, as demonstrated by preserved wound healing potency and intact ultrastructure in cryo-TEM analysis. The mild elution conditions, with EVs eluting at 400 mM NaCl, protect surface proteins and maintain critical quality attributes including size distribution, marker expression, and zeta potential across production batches.

From a manufacturing perspective, the disposable format eliminates column packing, cleaning validation, and cross-contamination risks while enabling closed-system processing compatible with GMP requirements. Processing times typically under one hour per batch translate directly into higher facility throughput and reduced buffer consumption.

The demonstrated linear scalability from 3 mL to 20 mL membrane volumes with maintained performance, combined with modular availability up to 4,800 mL, ensures that process transfer from development to clinical or commercial manufacturing requires only proportional adjustment of membrane area while holding residence time constant. This predictable scale-up behavior, confirmed through orthogonal analytics spanning particle counting, protein quantification, DNA clearance, and functional assays, dramatically simplifies process development timelines.

The analytical innovation presented here sets a foundation for future EV manufacturing development. The essential role of RT-MALS detection in visualizing EV fractions not detected by UV absorbance, the divergence between scattering-based and fluorescence-based particle counts distinguishing vesicular from non-vesicular populations, and the comprehensive integration of physical, biochemical, and functional characterization provide a roadmap for demonstrating product consistency to regulatory authorities. When integrated into complete downstream processing workflows comprising clarification, TFF concentration, IEX chromatography, buffer exchange, and sterile filtration, Sartobind Convec® D serves as the foundation of a fully scalable and reproducible purification platform.

For process development scientists and engineers advancing EV therapeutics toward clinical and commercial viability, Sartobind Convec® D provides a proven solution addressing the fundamental challenges of EV purification: selectivity, scalability, speed, and preservation of biological activity. The technology is ready for implementation in therapeutic development programs, offering the analytical and process understanding necessary for regulatory submission and commercial manufacturing. As the EV therapeutics field continues its rapid expansion with dozens of clinical trials underway and the first products approaching market authorization, Sartobind Convec® D helps address a key bottleneck in EV purification by supporting a controllable bioprocessing unit operation that enables EV-based medicines to reach patients.

For more information, visit
sartorius.com/en/applications/cell-and-gene-therapy/gene-therapy/extracellular-vesicles

References

1. Welsh, J. A., Goberdhan, D. C. I., O'Driscoll, L., Buzas, E. I., Blenkiron, C., Bussolati, B., Cai, H., Di Vizio, D., Driedonks, T. A. P., Erdbrügger, U., Falcon-Perez, J. M., Fu, Q. L., Hill, A. F., Lenassi, M., Lim, S. K., Mahoney, M. G., Mohanty, S., Möller, A., Nieuwland, R., Ochiya, T., ... Witwer, K. W. (2024). Minimal information for studies of extracellular vesicles (MISEV2023): From basic to advanced approaches. *Journal of Extracellular Vesicles, 13*(2), e12404. https://doi.org/10.1002/jev2.12404

2. Yu, L., Shi, H., Gao, T., Xu, W., Qian, H., Jiang, J., Yang, X., & Zhang, X. (2025). Exomeres and supermeres: Current advances and perspectives. *Bioactive Materials, 50,* 322–343. https://doi.org/10.1016/j.bioactmat.2025.04.012

3. Dehghani, M., Chai, M., Talebloo, N., Morrissey, M., Larey, A., Keselman, P., Rana, A., Islam, M., Mayo, M., Speidel, J., Mukherjee, P., Zhao, Z., Haridas, N., Marks, P., Chon, J., Kishimori, E., Gaborski, T., Kim, Y., Joshi, D., . . . Olszowy, M. (2026). Bioprocess design and optimization of extracellular vesicles derived from mesenchymal stromal cells. *ACS Nano.* https://doi.org/10.1021/acsnano.5c19046

Germany
Sartorius Stedim Biotech GmbH
August-Spindler-Strasse 11
37079 Göttingen
Phone +49 551 308 0

USA
Sartorius Stedim North America Inc.
565 Johnson Avenue
Bohemia, NY 11716
Toll-Free +1 800 368 7178

For more information, visit
sartorius.com

Last modified: 06 | 2026